



large glass window and a high voltage vacuum feedthrough. The chamber is also equipped with a 20  $\mu\text{m}$  Ti foil to absorb the electrons which can be positioned at the beam axis at different distances from the anode edge to allow beam emittance measurements. The electric signal from the foil is received through a feedthrough. The foil side opposite to the impinging beam is covered by a phosphor layer sensitive to X-rays and can be viewed by a CCD camera. To feed the gun a high voltage modulator with the pulse length about 10  $\mu\text{s}$  and repetition frequency varied in the range 1-50 Hz is used. It also provides the filament heating power. This regime of operation corresponds to that of the RTM.

### ELECTRON GUN TUNING

The geometry of the focusing electrode of the initial design and of the prototype version is shown in Fig. 1, the corresponding measured and simulated beam images are given in Fig. 3. As one can see, there is a considerable halo and the measured beam centre position is shifted upwards with respect to the axis for about 0.8 mm.

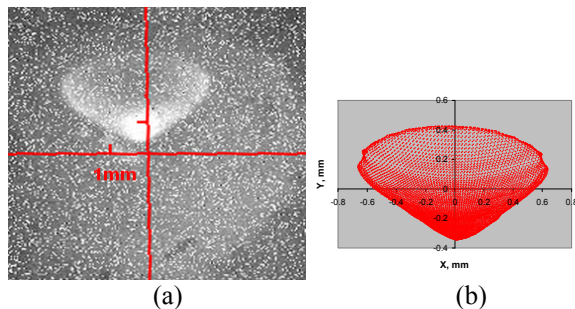


Figure 3: Registered and calculated beam image.

As a result of computer simulations it was found that the beam halo can be eliminated by placing a cylindrical conducting insertion in the cathode seat hole (see Fig. 4(a)) which produces a field with a local axial symmetry with respect to the cathode axis. The beam image registered after the installation of the insertion and optimization of its dimensions is shown in Fig. 4(b). We would like to note that in this case, due to a decrease of the field strength at the cathode surface, the gun current has diminished from  $\sim 30$  mA to  $\sim 25$  mA.

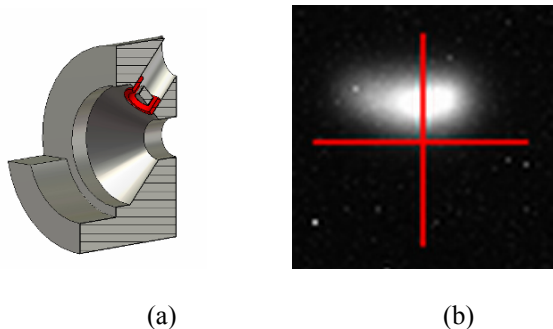


Figure 4: (a) Insertion in the cathode seat hole (shown in red). (b) Image of the beam from the gun with the insertion. The total length of each of the reference bars is 4 mm.

From computer simulations it was also found that to shift the beam position for 1 mm down towards the axis (see Fig. 3(a)) the length of the focusing electrode bulge must be decreased for about the same value. To check this we first cut the bulge for only 0.6 mm, as it is shown in Fig. 5(a). For a precise detection of the beam position shift the beam was generated at the maximal modulator repetition frequency which was sufficient for the beam to burn a hole in the foil (see Fig. 5(b)). The upper hole was burnt with the initial electrode design, the lower one after the bulge cut. As one can see, the beam position has shifted for about 0.6 mm well in accordance with the simulation prediction. After that the bulge has been cut for 0.2 mm more and the beam centre has set onto the horizontal axis.

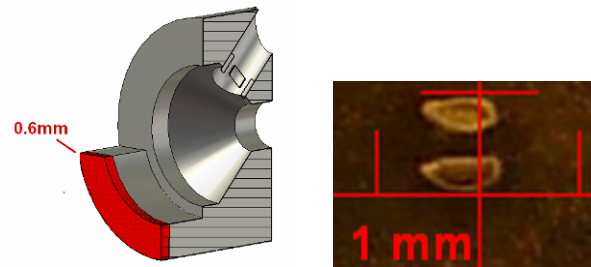


Figure 5: (a) Bulge cut which leads to the beam position shift downwards, (b) the holes burnt by the beam before and after the bulge cut.

### BEAM PARAMETER MEASUREMENTS

Estimates of rms beam parameters were done with the assumption that the beam had normal particle distribution in the horizontal and vertical transverse phase spaces and was described by rms ellipses and that the effect of the space charge forces on the free-space beam propagation was negligible.

Let  $\beta_{x,0}, \alpha_{x,0}, \gamma_{x,0}$  be horizontal optical functions (ellipse parameters) at some point  $z=z_0$  of the beam trajectory satisfying the standard relation  $\beta_{x,0}\gamma_{x,0} - \alpha_{x,0}^2 = 1$ . Then the rms beam size  $x_{rms}$  at some points  $z_i, i=0,1,2..N$  satisfies

$$\begin{aligned} x_{rms}^2(z_i) &= \beta_x(z_i) \varepsilon_{x,rms} = \\ &= \varepsilon_{x,rms} \left[ \beta_{x,0} - 2(z_i - z_0) \alpha_{x,0} + (z_i - z_0)^2 \gamma_{x,0} \right] \end{aligned} \quad (1)$$

(see, for example, [3]), where  $\varepsilon_{x,rms}$  is the rms beam emittance in the  $x$ -plane. Similar equations can be written for the  $y$ -plane. By measuring the rms beam sizes at least at three points and solving system of equations (1) the rms ellipse parameters at  $z_0$  and rms emittances can be obtained.

This procedure was applied by placing the Ti foil at  $z_0 = 15$  mm,  $z_1 = 30$  mm and  $z_2 = 45$  mm from the anode edge. Note, that  $z_0 = 15$  mm corresponds to the position of the entrance nose tip of the first accelerating cell of the RTM linac (Fig. 1) where the focusing force acting on the low energy injected beam is the strongest and where the

minimal beam dimensions are required. In Fig. 6 filtered beam images registered at  $z_0 = 15$  mm and  $z_2=45$  mm are shown. The filtering was used in order to remove a noise from the CCD matrix defects. With the data in the image binary file the rms horizontal and vertical beam dimensions at the measurement points were determined and the rms emittances and rms ellipse parameters at  $z_0 = 15$  mm were found. These results together with parameter values obtained in the computer simulation are listed in Table 1.

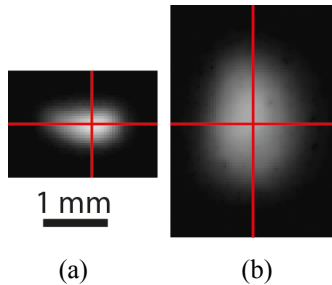


Figure 6: Filtered beam images at the distance 15 mm (a) and 30 mm (b) from the anode edge.

Table 1: Measured and Simulated rms Beam Parameters

Parameter	Measured	Calculated
$\epsilon_{x,rms}$ mm mrad	1.38	0.72
$\epsilon_{x,rms,norm}$ mm mrad	0.44	0.23
$\alpha_{x,0}$	-0.23	1.87
$\beta_{x,0}$ mm/mrad	0.08	0.07
$\epsilon_{v,rms}$ mm mrad	2.22	0.81
$\epsilon_{v,rms,norm}$ mm mrad	0.71	0.26
$\alpha_{v,0}$	-0.36	1.31
$\beta_{v,0}$ mm/mrad	0.01	0.01

As one can see from Table 1 the measured normalized rms emittances are quite small, less than 1 mm mrad, however they are about 2-3 times larger than the calculated values. The main reason for the discrepancy between the measured and calculated emittances can be a strong deviation of the phase space distributions from the normal ones with the elliptical boundary. In addition, the distribution in the  $y$ -plane is highly asymmetric. These discrepancies suggest that the method of the emittance reconstruction used here is too rough. Nevertheless, from the obtained results we can conclude that both the measured and calculated emittances are small enough, that the crossover of the emitted beam is at the required point and that the beam dimensions at the crossover fully satisfy the RTM beam dynamics requirements.

After the completion of the tests the electron gun was installed on the supporting platform inside the RTM vacuum chamber, as it is shown in Fig. 7.

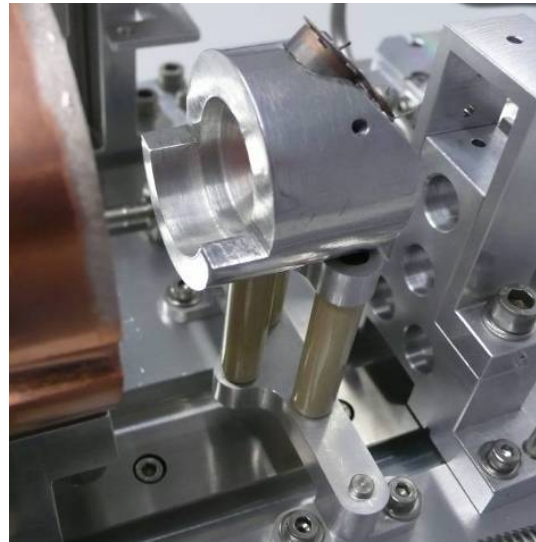


Figure 7: The electron gun installed on the RTM supporting platform.

## CONCLUSIONS

The engineering design of the definite optimized version of the electron gun for the compact RTM has been carried out. Its parts were manufactured and the gun was assembled and tested at a special stand. The results of the tests show that the electron gun fulfills required specifications. Also the vertical and horizontal emittances and beam ellipse parameters at the position of the first linac cell entrance were measured. The experimental values differ considerably from the simulated ones, most likely due to a non-Gaussian character of the particle phase space distribution of the emitted beam. Finally, the electron gun was installed inside the vacuum chamber of the RTM.

## REFERENCES

- [1] Yu.A. Kubyshin et al, "Current Status of the 12 MeV UPC Race-Track Microtron", PAC2-2009, Vancouver, May 2009, p. 2775.
- [2] A.V. Aloev, D. Carrillo, Yu.A. Kubyshin, N.I. Pakhomov, and V.I. Shvedunov, NIM A 624 (2010) 39.
- [3] H. Wiedemann, "Particle Accelerator Physics". Springer-Verlag, 1993.